Pak. J. Bot., 58(8) August 2026.

ARTICLE | **DOI: http://dx.doi.org/10.30848/PJB2026-8(7)**

ECO-FRIENDLY SYNTHESIS OF SILVER NANOPARTICLES FROM THE INVASIVE *NICOTIANA GLAUCA*: EXPLORING THEIR ANTIFUNGAL EFFICACY

AHMED M. ABBAS[1,3*], MAHMOUD FICTOR[2], MOHAMMED O. ALSHAHRANI[1], RAHMAH N. ALQTHANIN[1,3], ATTALLA F. EL-KOTT[1,4], SHAIMAA G. SALAMA[5], ZEINAB SAYED AHMED[1,3] AND MASSAUD MOSTAFA[6]

[1]Department of Biology, College of Science, King Khalid University, Abha, 61421, Saudi Arabia
[2]Department of Botany (Microbiology), Faculty of Agriculture, Qena University, Qena 83523, Egypt
[3]Prince Sultan Bin Abdulaziz for Environmental Research and Natural Resources Sustainability Center, King Khalid University, Abha 61421, Saudi Arabia
[4]Department of Zoology, Faculty of Science, Damanhour University, Egypt
[5]Department of Botany and Microbiology, Faculty of Science, Damanhour University, Damanhour 22511, Egypt
[6]Physics Department, Faculty of Science, Qena, Qena 83523, Egypt

*Corresponding author's email: ahhassan@kku.edu.sa

Abstract

This study explores the eco-friendly synthesis of silver nanoparticles (AgNPs) using an aqueous extract from the leaves of an invasive species *Nicotiana glauca*. The synthesized AgNPs were thoroughly characterized using X-ray diffraction (XRD), Fourier-transform infrared (FTIR) spectroscopy, dynamic light scattering (DLS), and transmission electron microscopy (TEM). DLS analysis confirmed the nanoparticles' monodispersity and stability, with an observed mean hydrodynamic diameter of 60.00 nm. XRD patterns indicated a face-centered cubic crystalline structure, with an average crystallite size of 42.58 nm. TEM imaging revealed that the nanoparticles were predominantly spherical, with sizes ranging from 50 nm to 55 nm. The AgNPs exhibited significant antifungal activity, with the largest inhibition zone measuring 26.0 mm against *Fusarium solani*, followed by 23.1 mm for *Aspergillus niger*. This study demonstrates that silver nanoparticles synthesized from *Nicotiana gl*auca leaf extract possess potent antifungal efficacy against key pathogens and exemplify a sustainable approach by valorizing an invasive plant for eco-friendly nanotechnolog Furthermore, this study highlights the innovative use of invasive plant species like *N. glauca* as a sustainable, environmentally friendly resource for nanoparticle production. By promoting green nanotechnology, this work contributes to biodiversity conservation efforts while providing a practical approach to managing invasive alien plants.

Key words: Invasive; Green source; SEM; FTIR; Silver

Introduction

Nanotechnology is an advanced field with great potential to benefit human health. The main focus in this field is on the production of nanoparticles with precise control over their size, shape, chemical composition, and dispersion to improve their use in various fields (Mohanpuria *et al.,* 2008). Standard methods for producing nanoparticles include physical, chemical, and biological methods. While physical and chemical techniques can create well-defined nanoparticles, they are often costly and environmentally harmful (Bhattacharya & Gupta, 2005 ; Bachheti *et al.,* 2022). For these reasons, environmentally friendly alternatives have been developed, with green synthesis emerging as a sustainable, cost-effective, and scalable solution for producing nanoparticles (Dhuper *et al.,* 2012). This approach eliminates the need for toxic chemicals, reduces energy consumption, and avoids hazardous chemicals, providing an environmentally friendly method for large-scale production (Roy, 2015). Metallic nanoparticles, especially silver nanoparticles (AgNPs), have gained interest due to their exceptional optical, magnetic, and catalytic properties (Suganthy *et al.,* 2018; Bachheti *et al.,* 2021). These nanoparticles have tunable size, high dispersibility, stability, biocompatibility, and superior adsorption capabilities. Silver nanoparticles (AgNPs) are considered among the most promising for various biological applications (Wang *et al.,* 2021; Manjari *et al.*, 2017; Husen *et al.,* 2019; Singh *et al*., 2018).

Biological methods are widely used and preferred for the reasons mentioned above. As a result, numerous commercial AgNPs products are currently available (Vance *et al.*, 2015). Silver nanoparticles (AgNPs) remain one of the most extensively utilized metal nanoparticles, finding applications in various fields including wastewater treatment (Suganthy *et al.,* 2018), electronics (Bachheti *et al.,* 2021; Wang *et al.,* 2021; Manjari *et al.,* 2017), DNA labeling (Husen *et al.,* 2019; Singh *et al.,* 2018; Vance *et al.,* 2015), filtration systems (Kalishwaralalf *et al.*, 2010; Joshi *et al.,* 2016), sensor technology (Mcconnachie *et al.,* 2011; Tamado & Milberg, 2000), antimicrobial coatings. Leyu *et al*., 2023; Salayová *et al*., 2021; Rawat, 2017) , and as antimicrobial agents (Rawat *et al*., 2023; Singh *et al.,* 2003; Lakshmi *et al.*, 2007).

Received: 15-11-2025 | Revised: 26-01-2026 | Accepted: 30-01-2026 | Online: 01-04-2026

These nanoparticles are produced using various physical, chemical, and biological techniques. Among the different biological methods for synthesizing nanoparticles, microbe-mediated synthesis is not commercially feasible due to the need for strict aseptic conditions and ongoing maintenance. Plant extracts are favored over microorganisms for this purpose because they are easier to scale up, pose less of a biohazard, and do not require cell culture maintenance (Kalishwaralal *et al.*, 2010). Therefore, it is an interesting idea to explore the potential of the invasive plant species, *N. glauca*, for the production of nanoparticles in Saudi Arabia. In many experiments, various chemicals are introduced to initiate reactions, with sodium hydroxide commonly used to modify pH or facilitate nanomaterial synthesis. However, our method did not add any external substance; instead, we utilized only the plant extract and the salt designated for nanomaterial preparation, successfully attaining the intended results.

Nicotiana glauca Graham is a perennial shrub belonging to the Solanaceae family. It is native to northwest Argentina and Bolivia but has become a fast-growing invasive species in many countries, including the United States, Mexico, South Africa, Namibia, Morocco, Egypt, Saudi Arabia, Australia, and Croatia (Lakshmi & Srinivas, 2007; Issaly *et al.*, 2020). Anthropogenic activities are responsible for its spread, it has alongwith it ability to grow well in warm, temperate regions (Florentine *et al.,* 2006). This species is listed as invasive in both the Global Invasive Species Database (GISD) and the Invasive Species Compendium (CABI) (Florentine *et al.,* 2006). *N. glauca* is highly adaptable, growing across a wide range of elevations and soil types, where it can quickly establish dense, monospecific populations (Florentine *et al.,* 2006). It often colonizes disturbed areas such as roadsides, rocky terrains, arid grasslands, coastal zones, and other degraded habitats (Nattero & Cocucci, 2007). Moreover, the plant faces limited predation due to its production of anabasine, a toxic alkaloid harmful to humans and animals (Scharenberg *et al.,* 2019). In recent decades, many non-native plant species have spread extensively across Saudi Arabia, especially in the southwestern region, which hosts 74% of the country's plant species. Among these, *N. glauca* is regarded as one of the most aggressive invasive species, able to grow at elevations ranging from 800 to 2700 m a.s.l. (Thomas *et al.,* 2016). Although its impact is significant, no previous studies have attempted to utilize this plant through environmentally friendly, non-chemical methods.

The aim of this study was to synthesize and characterize silver nanoparticles (AgNPs) using the invasive plant *N. glauca* through an eco-friendly green synthesis method and to evaluate their antifungal activity. Most probably, this has not been investigated previously.

Materials and Methods

Plant materials: Fresh *Nicotiana glauca* leaves were harvested from a rangeland farm (18°08′05″ N, 42°42′26″ E) (Fig. 1). The collected leaves were dried in an oven at 60°C for 48 hours. The plant species was taxonomically identified by the Herbarium of the Biology Department at King Khalid University.

Preparation of *N. glauca* extract: The plant material was properly washed with distilled water after being repeatedly washed with tap water to eliminate impurities and visible contaminants. Then, it completely dried in the shade. The dried plant material was crushed into a fine powder using a mortar and pestle. About 20 g of cleaned *N. glauca* leaves were placed in 200 mL of boiled distilled water for ~1 hour at 50°C using a magnetic stirrer. After the mixture cooled to room temperature, it was centrifuged for 10 minutes at 6000 rpm, and the supernatant was decanted. The extract mixture was filtered through of Whatman No. 1. filter paper. The clear supernatant solution was collected and stored at 4ºC (Latha *et al.,* 2019).

Fig. 1. *Nicotiana glauca* tree with flowering shoots.

Synthesis of the silver oxide nanoparticles: The silver nitrate (2.5 g) was dissolved in distilled water and then treated with plant extract under sunlight using a magnetic stirrer at 50ºC. The solution turned deep red, confirming AgNPs formation.. The mixture was centrifuged at 6000 rpm for 10 min and washed once with distilled water and ethanol to remove residual extract.

Characterization of the synthesized Ag-based nano particles

X-ray Diffraction (XRD): X-ray diffraction was utilized to examine the formation and quality of the synthesized AgNPs . The AgNPs were centrifuged (1400 rpm; 8ºC) for 15 min, then washed three times in ethanol before being washed three times with sterile Milli-Q water. The AgNPs were then purified and ground using a ceramic mortar and pestle in a 60ºC oven. An X-ray diffractometer (X'Pert PROPAN Analytical, Europe) was used to analyze the powdered sample of characteristic Co-Kα radiation (λ = 1.78 Å) over a range of 20º to 90º, with a scan rate of 0.05º /min and a time constant of 2 second.

Fourier-transform infrared spectroscopy (FT-IR): FT-IR spectroscopy was used to detect the functional groups associated with the reduction of Ag ions and the capping of reduced Ag oxide nanoparticles. Shimadzu infrared (IR) double-beam spectrophotometer was used for recording the FT-IR spectrum of dried silver nanoparticles (NPs) in transmittance mode. The samples were prepared using the potassium bromide (KBr) pellet method at a 1:30 ratio (NPs:KBr). The resulting spectral peaks, indicative of molecular stretching, were plotted with transmittance on the Y-axis and wavenumber (cm^{-1}) on the X-axis. The spectrum was recorded in the wavenumber range of 500–4500 cm^{-1}, and a baseline correction was applied by subtracting the spectrum of pure KBr.

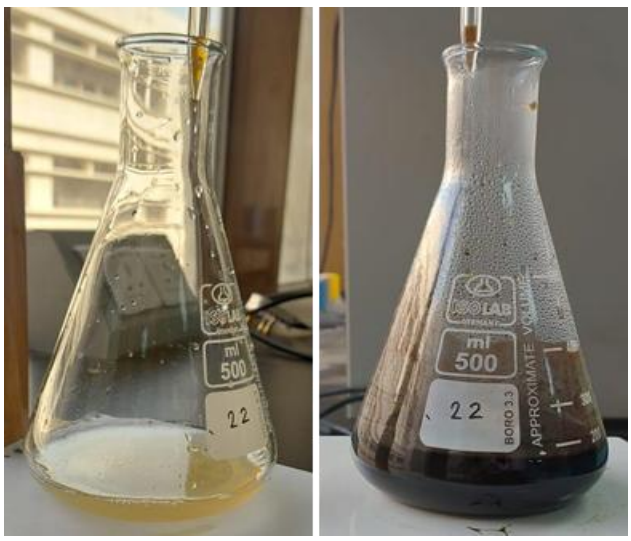

Fig. 2. The color change of solution after the reduction of AgNO3 by *N. glauca* leaf extract.

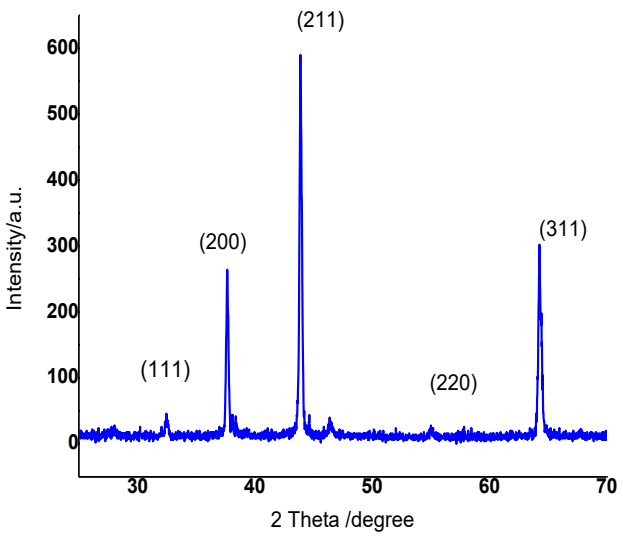

Fig. 3. XRD- the pattern of biogenically synthesized AgNPs nanoparticles (NPs).

Transmission electron microscopy (TEM): Transmission electron microscopy (TEM (JEM-1230, JEOL, Akishima, Japan)) was used to examine the structural characteristics and particle size of the NPs. A drop of NP-containing solution was placed on carbon-coated copper grids, for 1 min to form a thin film. Excess liquid was then removed using filter paper, and the grids were vacuum-dried overnight before being loaded into a specimen holder for analysis (Nasiriboroumand *et al.,* 2018).

SEM analysis: Scanning electron microscopy (SEM) analysis was conducted using a Carl Zeiss Japan model. A thin film of the nanoparticle powder was prepared on carbon-coated tape, with a small amount of dried fine powder adhered to the grid. Excess material was carefully removed using blotting paper. After exposure to a mercury lamp for 5 minutes, the film on the SEM grid was left to dry completely. The surface structure of the biogenically synthesized silver nanoparticles (Ag NPs) was then examined through SEM analysis.

***In vitro* antifungal activity of AgNPs:** The antifungal activity of AgNPs was evaluated using agar well diffusion against *Aspergillus niger* RCMB 02724, and *Fusarium solani* SX13. All tested fungal strains were grown on PDA plates and incubated for 3–5 days at 30°C (Hashem *et al.,* 2021; Khalil & Hashem, 2018). The fungal suspension was prepared in sterilized phosphate buffer solution (PBS) pH 7.0, and then the inoculum was adjusted to 10^7 spores/mL after counting in a cell counter chamber. One milliliter was uniformly distributed on agar PDA plates, which acted as the positive control. Using a sterile cork-borer, wells (8 mm) were cut; agar MEA was first loaded with 100 mL of plant extract, and AgNPs were transferred to each well individually and left for 2 h at 4°C, and then the plates were incubated for 3 days at 30°C. Moreover, concentrations of 125, 250, and 500 µg/ mL of AgNPs were evaluated, and after incubation, the inhibition zones were determined.

Results

Visual examination: The transformation in color from light yellow to deep brown confirmed clear visual evidence for the synthesis of silver nanoparticles. This color transition was observed within 30 minutes of exposure, as shown in Fig. 2.

The XRD analysis confirms the presence of characteristic AgNPs diffraction peaks, thus validating the wurtzite crystal structure of the nanoparticles. The peaks observed at 32.49°, 37.64°, 46.44°, 55.00°, 64.26°, and 77.34° correspond to the (111), (2 0 0), (2 1 1), (2 2 0), (3 1 1), and (3 2 1) planes of AgNPs, respectively (Fig. 3). The XRD diffraction peaks align exclusively with the face-centered cubic (FCC) structure of metallic silver (Ag^0), as confirmed by comparison with standard reference data (JCPDS 04-0783). No evidence of silver oxide or other crystalline phases was observed, indicating complete reduction of Ag^+ ions to elemental silver by the phytochemicals present in the *Nicotiana glauca* extract. These results are consistent with established green synthesis mechanisms, where plant-derived biomolecules facilitate the formation and stabilization of zero-valent silver nanoparticles.

The calculated crystalline size of the AgNPs, the strain, and cell parameters are presented in Table 1. The crystallite size of the prepared AgNPs was determined to be around 42.58 nm; also, lattice parameters (a, b, c) were measured to be about 4.718.

Table 1. The lattice constant values for the samples.

Sample	a=b=c	c/a	strain	Crystallite size
AgNPs	4.718	1	0.27	42.58 nm

Structure refinements: The atomic positions of the biogenically synthesized AgNPs were determined via X-ray powder diffraction utilizing the Rietveld refinement technique. The position of the silver atoms was found to correlate with the oxygen content. The FULLPROF software, designed for Rietveld-type analysis, facilitated the least-squares structural refinements. Fig. 4 illustrates the observed, calculated, and various profiles resulting from the final Rietveld refinement of the AgNPs. The blue line in the figure represents the correspondence between the experimental data and the model during the refinement process. The analysis used the Pn-3m space group

appropriate for cubic structures. To fit the parameters of the X-ray diffraction data, the pseudo-Voigt function was used. The refining parameters for the biogenically produced AgNPs including occupancy, atomic positions, crystal system, space group, lattice parameters, and cell volume, are summarized in Table 2. The lattice constants (a, b, and c) were determined to be ~ 4.8, and the cell volume was 105.02 Å.

FTIR Analysis: Various biomolecules essential for coating and stabilizing reduced silver nanoparticles (AgNPs) and reducing silver ions (Ag+) were identified using FTIR analysis. Fig. 5. revealed intense absorption peaks are detected at 2918 cm^{-1}, 2364 cm^{-1}, 2202 cm^{-1}, 1580 cm^{-1}, and 655 cm^{-1} with a wavelength range of 500–4000 cm^{-1}. These results indicate the presence of important functional groups from the plant extract in the synthesized nanoparticles, confirming the stabilization and reduction of AgNPs made by the plant extract. The FTIR spectrum of the synthesized AgNPs represented in Fig. (5) displayed minor alterations in both peak position and intensity. The shift observed at 2918.88 cm^{-1} could be indicative of hydrogen bond disruption, which is important in the reduction process of silver ions to form silver nanoparticles.

TEM study of nanoparticle: The morphological characteristics of the biosynthesized silver nanoparticles (AgNPs), including their size, shape, and other features, were analyzed using transmission electron microscopy (TEM). TEM images of the nanoparticles are presented in (Fig. 6a). The measurements obtained from these images indicated that the sizes of the AgNPs range from 45 to 75 nm (Fig. 6a). Differences in particle size were observed when comparing the sizes obtained from TEM with those from dynamic light scattering (DLS) analysis.

Table 2. Final Rietveld refinement parameter of Cubic AgNPs.

Compound	Space group	a=b=c (Å)	α=β= γ	η=c/a	Cell volume (Å)	Atom	x	y	z
Ag_2O	Pn^{-3m}	4.8	90°	1	105.02	Ag O	0.25 0.00	0.25 0.00	0.25 0.00

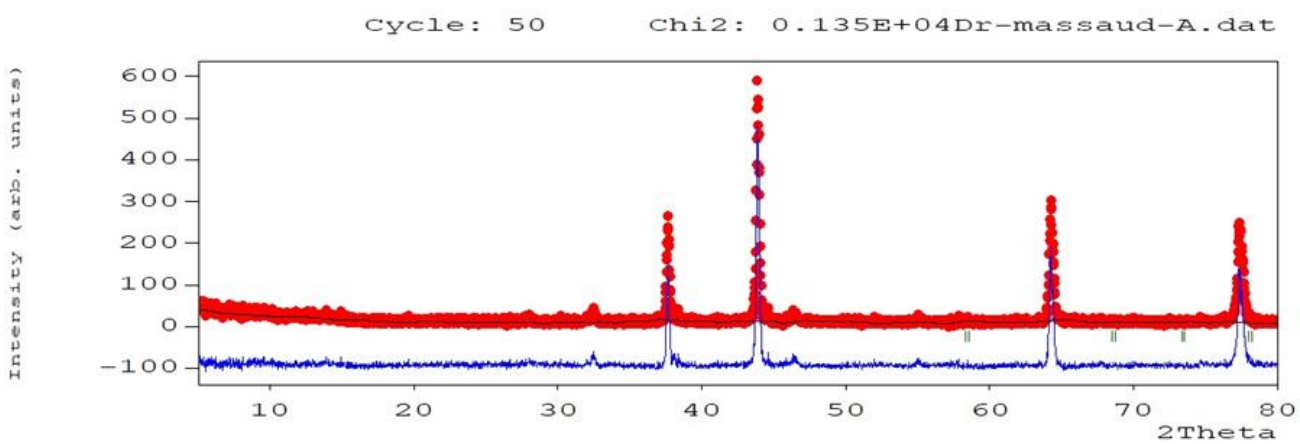

Fig. 4. Rietveld refinement results of cubic structure of AgNPs.

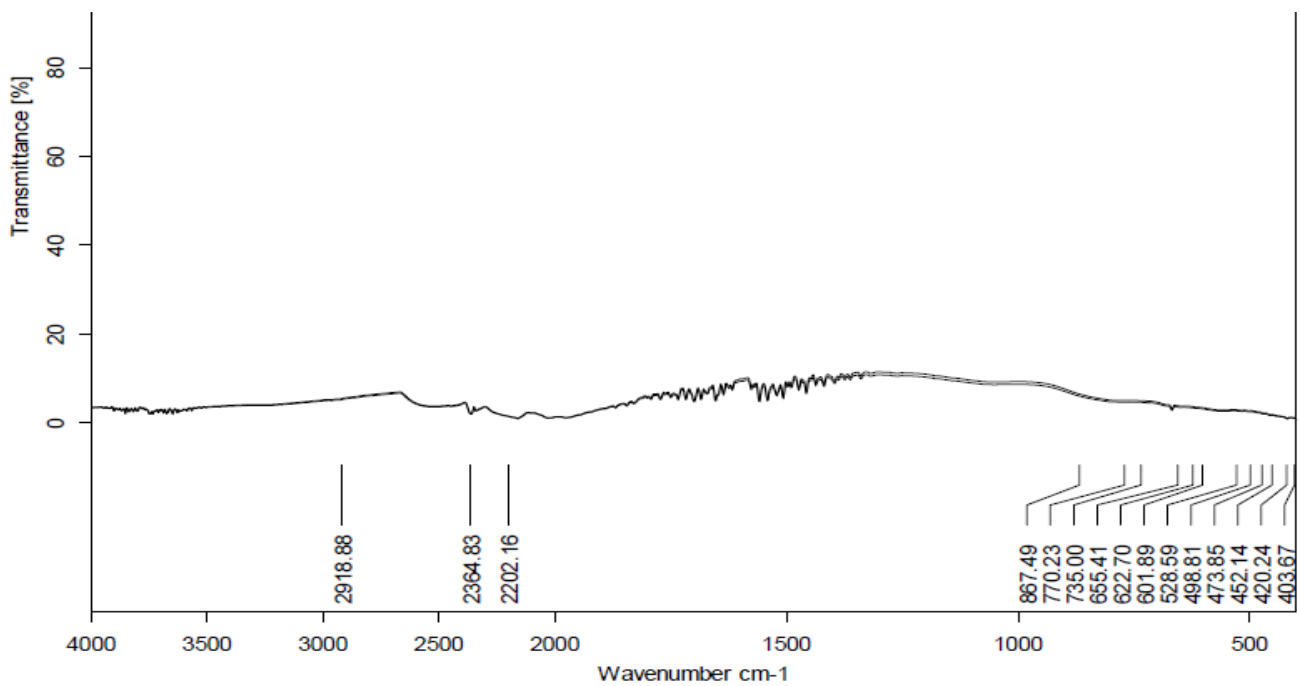

Fig. 5. FTIR spectra of biosynthesized AgNPs.

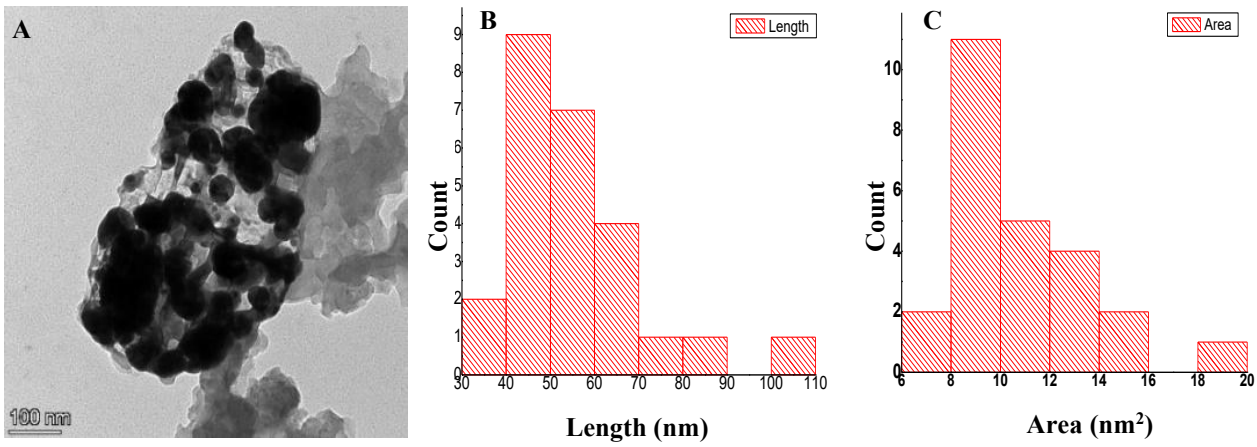

Fig. 6. TEM image (a) the particle size distribution histogram (b) and the area distribution histogram (c).

Figure 6 (b and c) present histograms showing the particle size distribution for nb- AgNPs and Np- AgNPs, respectively. The average particle size of Np-Ag_2O ranges from 50 to 55 nm, with an average area of 2000 to 3000 nm². Furthermore, the transmission electron microscopy (TEM) image of Np- AgNPs shown in Fig 6(a) indicates that this material has a high level of crystallinity.The difference between TEM (50-55 nm) and DLS (60 nm) is slight and may be due to the process of aggregation of silver nanoparticles, which gives them a larger size.

SEM: The morphology and distribution of the synthesized silver nanoparticles (AgNPs) were analyzed using Field Emission Scanning Electron Microscopy (SEM). SEM images captured at scales of 10 µm and 42.48 nm, with magnifications of 25,000×, 50,000×, and 100,000× respectively, revealed spherical, polydisperse nanoparticle aggregates (Fig. 7).

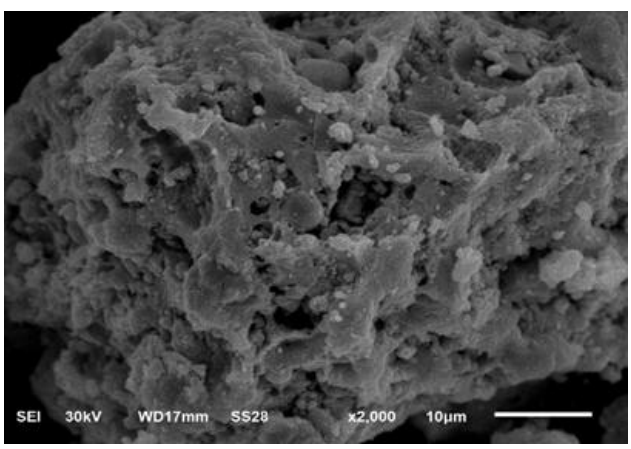

Fig. 7. Scanning electron microscope (SEM) images of synthesized AgNPs at 10 µm.

The crystal structure of cubic AgNPs: As shown in (Fig. 7), the final Rietveld refinement parameters were employed to standardize the crystal structure and fractional coordinates using the VESTA (Visualization for Electronic and Structural Analysis) program. Ag nanoparticles (NPs) have a well-established cubic crystal structure characterized by the space group Pn-3m. The hexagonal unit cell of the wurtzite structure features two lattice parameters, (a) and (c), with the ratio c/a = 1, which is typical for an ideal wurtzite configuration. Figure 8 presents a schematic representation of the cubic AgNPs structural model based on the final Rietveld refinement parameters. This structure consists of two interpenetrating hexagonal close-packed (hcp) sublattices, each formed by one type of atom that is displaced by u = 3/8 = 0.375 along the three-fold axis of the c-axis, as detailed in Table 2 (in an ideal cubic structure) in fractional coordinates. The internal parameter u is defined as the length of the link parallel to the c-axis (the anion–cation bond length or nearest-neighbor distance) divided by the c lattice parameter.

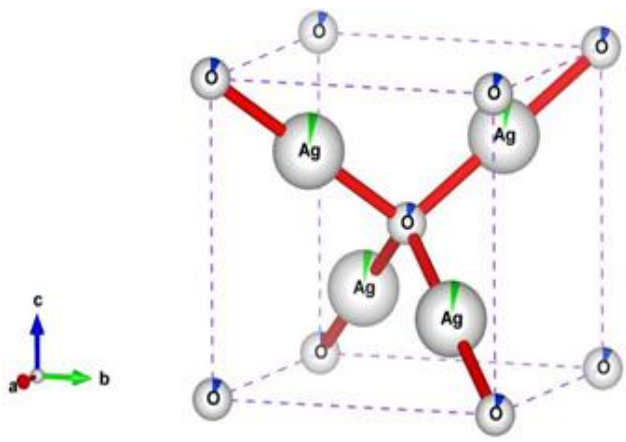

Fig. 8. Schematic model of cubic AgNPs structure with lattice constants a, b and c.

Antifungal activity: *Aspergillus niger* demonstrated a higher sensitivity to both plant extracts and AgNPs compared to *Fusarium solani*. The highest inhibition zone (26.4 ± 0.43 mm) was observed for *Aspergillus niger* at 500 µg/mL of AgNPs (Table 3). For *Aspergillus niger*, the zone of inhibition produced by the plant extract was 12.3 ± 0.13 mm, while AgNPs at concentrations of 125 µg/mL, 250 µg/mL, and 500 µg/mL produced zones of 13.4 ± 0.18 mm, 17.5 ± 0.50 mm, and 26.4 ± 0.43 mm, respectively (Table 3). Similarly, for *Fusarium solani*, the plant extract exhibited a zone of inhibition of 11.2 ± 0.11 mm, and AgNPs at 125 µg/mL, 250 µg/mL, and 500 µg/mL showed inhibition zones of 10.0 ± 0.12 mm, 15.1 ± 0.42 mm, and 23.4 ± 0.14 mm, respectively (Table 3).

Table 3. Zone of inhabitation produced (mm), of plant extract, and AgNPs at concentration125, 250 and 500 µg/mL against *Aspergillus niger* and *Fusarium solani*.

Microorganisms	Zone of inhibition produced (mm)			
	Plant extract	AgNPs (µg/ mL)		
		125	250	500
Aspergillus niger	12.3 ± 0.13	13.4 ± 0.18	17.5 ± 0.50	26.4 ± 0.43
Fusarium solani	11.2 ± 0.11	10.0 ± 0.12	15.1 ± 0.42	23.4 ± 0.14

These results indicate that AgNPs exhibit a concentration-dependent increase in antimicrobial activity. Furthermore, this suggests that AgNPs are more effective against fungal pathogens at higher concentrations (Table 3).

Discussion

The observed color change can be attributed to surface plasmon resonance (SPR), as evidenced by biogenically reduced silver nanoparticles (AgNPs) (Ahsan & Farooq, 2019). These results agree with previous studies by Erdogan *et al*., (2016), and Moreno, (2018). The results revealed a specific and sharp peak, indicating that the formed particles had a well-crystallized structure and metallic nature (Pourzahedi *et al.*, 2017; Alsamhary, 2020). The strong intensity of these diffraction peaks underscores the crystalline nature of the AgNPs (Shu *et al.,* 2020). The diffraction peaks observed can be attributed to the cubic structure, specifically reflecting the pure Bragg's reflections characteristic of the face-centered cubic (FCC) arrangement found in metallic silver powder (Khalil *et al.,* 2014). these results agreed with the Joint Committee on Powder Diffraction Standards (JCPDS) standard No. 04-0783. (Leyu *et al.,* 2023) documented successfully synthesized crystalline silver nanoparticles (AgNPs) through reducing silver ions using the invasive alien species *Parthenium hysterophorus*, characterized by face-centered cubic structures. These results agree with the previous work; the average crystallite size of the AgNPs nanoparticles was determined using the Debye–Scherrer equation (Mostafa *et al.,* 2020).

$$t = 0.9\lambda/\beta Cos\theta \qquad (1)$$

Where λ is the wavelength, β is the full width at half maximum (FWHM), and θ is the diffraction angle.

The final Rietveld refinement analysis indicates that AgNPs have a cubic structure and high crystallinity (Mobarak *et al.,* 2020). Results revealed intense absorption peaks are detected at 2918 cm^{-1}, 2364 cm^{-1}, 2202 cm^{-1}, 1580 cm^{-1}, and 655 cm^{-1} with a wavelength range of 500–4000 cm^{-1} (Oluwaniyi *et al.,* 2016). The peak at 29180.88 cm^{-1} is Caused by C–H stretching vibrations, while the peaks at 2364.83 cm^{-1} and 2202.16 cm^{-1} are Combined with C=O stretching and N–H bending modes in primary amides (Awwad *et al.,* 2013). The stretching mode for the carbonyl group (C=O) was detected at 1580 cm^{-1}, indicating the presence of compounds such as carboxylic acids, aldehydes, esters, or ketones derived from flavonoids and tannins (Kumar *et al.,* 2019). The main peak observed at 2918 cm^{-1} could be attributed to the OH stretching group of phenols and alcohols or the NH stretching of aliphatic primary amines (Jalali *et al.,* 2020). Also, the spectral patterns of the plant leaf extract and the synthesized AgNPs Similar to each other, suggesting that the identified phytochemicals are present in the synthesized nanoparticles (Javan *et al.,* 2020).

This variation is due to the aggregation of the nanoparticles, which affects the accuracy of the DLS measurements. The presence of larger particles increases light scattering, inflating the measured particle size (Souza *et al.,* 2016). TEM images confirm that most of the nanoparticles exhibit a spherical morphology. SEM images captured at scales of 10 µm and 42.48 nm, with magnifications of 25,000×, 50,000×, and 100,000× respectively, revealed spherical, polydisperse nanoparticle aggregates (Amargeetha & Velavan 2018). The final Rietveld refinement parameters were employed to standardize the crystal structure and fractional coordinates using the VESTA (Visualization for Electronic and Structural Analysis) program (Momma & Izumi, 2011). Previous studies showed that antifungal activities were determined in broth dilution bioassay (Pujol *et al*., 1996; Irkin & Korukluoglu, 2009). Similarly, for *Fusarium solani*, the plant extract exhibited a zone of inhibition of 11.2 ± 0.11 mm, and AgNPs at 125 µg/mL, 250 µg/mL, and 500 µg/mL showed inhibition zones of 10.0 ± 0.12 mm, 15.1 ± 0.42 mm, and 23.4 ± 0.14 mm, respectively (Singh *et al*., 2024).The successful green synthesis of AgNPs using *N. glauca* is confirmed by characteristic SPR and XRD patterns, showing well-crystallized, cubic nanoparticles with a size comparable to those from other invasive plants (Leyu *et al*., 2023). The AgNPs exhibited strong, concentration-dependent antifungal activity, with inhibition zones up to 26.4 mm against *A. niger*. This efficacy surpasses that of AgNPs from *Carya illinoinensis* (Javan *et al*., 2020) and matches the potency of *Prunus serrulata*-synthesized AgNPs (Kim, 2018). The antifungal action is primarily attributed to ROS generation and Ag^+ ion release, which disrupt fungal membranes and cause oxidative stress (Suganthy *et al*., 2018; Singh *et al*., 2024). Phytochemicals from the extract, identified by FTIR, likely enhance this mechanism through synergistic capping. Ecologically, this work valorizes *N. glauca* a highly invasive species threatening biodiversity (Thomas *et al*., 2016) by transforming it into a nanomaterial resource. This approach supports sustainable invasive species management through biorefining, aligning with circular economy principles (Rawat *et al*., 2023). Thus, the study provides both an effective antifungal agent and a practical strategy for ecological conservation.

Conclusion

This study successfully demonstrates the viability of *Nicotiana glauca* leaf extract for the sustainable, green synthesis of silver nanoparticles (AgNPs). The characterization confirmed the formation of well-defined, crystalline AgNPs suitable for functional applications. The findings underscore the significant translational potential of these nanoparticles in agricultural and biomedical fields. As a potent antifungal agent, the synthesized AgNPs could be developed into eco-friendly formulations for crop protection against pathogenic fungi such as *Aspergillus niger* and *Fusarium solani*, reducing reliance on synthetic fungicides. Furthermore, their inherent antimicrobial properties position them as promising candidates for biomedical applications, including wound dressings, antibacterial coatings,

and therapeutic nanosystems. Beyond material innovation, this work establishes a circular model for invasive species management by converting *N. glauca* an ecological threat into a valuable resource for nanotechnology. This approach not only advances green synthesis but also contributes to environmental conservation, offering a dual-purpose strategy that aligns with sustainable development goals. Future work should focus on scaling production, conducting in vivo efficacy and safety studies, and exploring integrated applications in agri-biotechnology and healthcare.

Acknowledgments

The authors extend their appreciation to the Deanship of Research and Graduate Studies at King Khalid University for funding this work through a Large Group Project under grant number (RGP. 2/440/46).

References

Ahsan, A. and M.A. Farooq. 2019. Therapeutic potential of green synthesized silver nanoparticles loaded PVA hydrogel patches for wound healing. *J. Drug Deliv. Sci. Technol.*, 54: 101308, doi:10.1016/j.jddst.2019.101308.

Alsamhary, K.I. 2020. Eco-friendly synthesis of silver nanoparticles by *Bacillus subtilis* and their antibacterial activity. *Saudi J. Biol. Sci.*, 27: 2185-2191, doi:10.1016/j.sjbs.2020.04.026.

Amargeetha, A. and S. Velavan. 2018. X-Ray Diffraction (XRD) and energy dispersive spectroscopy (EDS) analysis of silver nanoparticles synthesized from *Erythrina indica* flowers. *Nanosci. Technol.*, *5*: 1-5.

Awwad, A.M., N.M. Salem and A.O. Abdeen. 2013. Green synthesis of silver nanoparticles using carob leaf extract and its antibacterial activity. *Int. J. Ind. Chem.,* 4: 1-6.doi:10.1186/2228-5547-4-29

Bachheti, A., R.K. Bachheti, L. Abate and A. Husen. 2022. Current status of aloe-based nanoparticle fabrication, characterization and their application in some cutting-edge areas. *S. Afr. J. Bot.*, 147: 1058-1069.

Bachheti, R.K., L. Abate, A. Deepti Bachheti, A. Madhusudhan and A. Husen. 2021. Algae-, fungi-, and yeast-mediated biological synthesis of nanoparticles and their various biomedical applications. In: *Handbook of Greener Synthesis of Nanomaterials and Compounds: Volume 1: Fundamental Principles and Methods*; Elsevier, pp. 701-734 ISBN 9780128219386.

Bhattacharya, D. and R.K. Gupta. 2005. Nanotechnology and potential of microorganisms. *Crit. Rev. Biotechnol.*, 25: 199-204.

Dhuper, S., D. Panda and P.L. Nayak. 2012. Green synthesis and characterization of zero valent iron nanoparticles from the leaf extract of *Mangifera indica*. *Nano Trends J. Nanotech. App.,* 13: 16-22.

Erdoğan, T., F.F. Yılmaz, B. Kıvçak and M. Özyazıcı. 2016. Green synthesis of silver nanoparticles using arbutus andrachne leaf extract and its antimicrobial activity. *Trop. J. Pharm. Res.*, 15: 1129-1136.

Florentine, S.K., M.E. Westbrooke, K. Gosney, G. Ambrose and M. O'Keefe. 2006. The arid land invasive weed *Nicotiana glauca* R. Graham (Solanaceae): Population and soil seed bank dynamics, seed germination patterns and seedling response to flood and drought. *J. Arid Environ.*, 66: 218-230.

Hashem, A.H., A.M.A. Khalil, A.M. Reyad and S.S. Salem. 2021. Biomedical applications of mycosynthesized selenium nanoparticles using *Penicillium expansum* ATTC 36200. *Biol. Trace Elem. Res.*, 199: 3998-4008.

Husen, A., Q.I. Rahman, M. Iqbal, M.O. Yassin and R.K. Bachheti. 2019. Plant-mediated fabrication of gold nanoparticles and their applications. In *Nanomaterials and Plant Potential*; Springer: Berlin/Heidelberg, Germany, pp. 71–110 ISBN 9783030055691.

Irkin, R. and M. Korukluoglu. 2009. Effectiveness of *Cymbopogon citratus* L. essential oil to inhibit the growth of some filamentous fungi and yeasts. *J. Med. Food*., 12: 193-197.

Issaly, E.A., A.N. Sérsic, A. Pauw, A.A. Cocucci, A. Traveset, S.M. Benítez-Vieyra and V. Paiaro. 2020. Reproductive ecology of the bird-pollinated *Nicotiana glauca* across native and introduced ranges with contrasting pollination environments. *Biol. Invas.*, 22: 485-498.

Jalali, E., S. Maghsoudi and E. Noroozian. 2020. A novel method for biosynthesis of different polymorphs of TiO2 nanoparticles as a protector for *Bacillus thuringiensis* from Ultra Violet. *Sci. Rep.*, 10: 426.doi:10.1038/s41598-019-57407-6

Javan, B.D.S., H. Djahaniani, F. Nabati and M. Hekmati. 2020. Characterization and the evaluation of antimicrobial activities of silver nanoparticles biosynthesized from *Carya illinoinensis* leaf extract. *Heliyon*., 6: e03624,

Joshi, A., R.K. Bachheti, A. Sharma and R. Mamgain. 2016. *Parthenium hysterophorus*. L.(Asteraceae): A Boon or Curse? (A Review). *Orient. J. Chem.*, 32: 1283.doi.org/10.13005/ojc/320302

Kalishwaralal, K., V. Deepak, S.R.K. Pandian, M. Kottaisamy, S. BarathManiKanth, B. Kartikeyan and S. Gurunathan. 2010. Biosynthesis of silver and gold nanoparticles using *Brevibacterium casei*. *Colloids surfaces B Biointerfaces*, 77: 257-262.

Khalil, M.A. and A. H. Hashem. 2018. Morphological Changes of Conidiogenesis in Two *Aspergillus* species. *J. Pure Appl. Microbiol.*, 12: 2041-2048.

Khalil, M.M.H., E.H. Ismail, K.Z. El-Baghdady and D. Mohamed. 2014. Green synthesis of silver nanoparticles using olive leaf extract and its antibacterial activity. *Arab. J. Chem.*, 7: 1131-1139.

Kim, Y.J. 2018. *In vitro* anti-inflammatory activity of spherical silver nanoparticles and monodisperse hexagonal gold nanoparticles by fruit extract of *Prunus serrulata*: A green synthetic approach. *Artif. Cells, Nanomed. Biotechnol.*, 46: 2022-2032.

Kumar, V., S. Singh, B. Srivastava, R. Bhadouria and R. Singh. 2019. Green synthesis of silver nanoparticles using leaf extract of *Holoptelea integrifolia* and preliminary investigation of its antioxidant, anti-inflammatory, antidiabetic and antibacterial activities. *J. Environ. Chem. Eng.*, 7, 103094.doi:10.1016/j.jece.2019.103094

Lakshmi, C. and C. Srinivas. 2007. Parthenium: A wide angle view. In: *Proceedings of the Indian Journal of Dermatology, Venereology and Leprology.,* Vol. 73: pp. 296-306.doi: 10.4103/0378-6323.35732

Latha, D., P. Prabu, G. Gnanamoorthy, S. Sampurnam, R. Manikandan, C. Arulvasu and V. Narayanan. 2019. *Facile Justicia adhatoda* leaf extract derived route to silver nanoparticle: Synthesis, characterization and its application in photocatalytic and anticancer activity. *Mater. Res. Express*., 6, 45003.doi:10.1088/2053-1591/aaf828

Leyu, A.M., S.E. Debebe, A. Bachheti, Y.S. Rawat and R.K. Bachheti. 2023. Green synthesis of gold and silver nanoparticles using invasive alien plant *Parthenium hysterophorus* and their antimicrobial and antioxidant activities. *Sustain.*, 15, doi:10.3390/su15129456.doi:10.3390/su15129456

Manjari, G., S. Saran, T. Arun, S.P. Devipriya and A. Vijaya Bhaskara Rao. 2017. Facile *Aglaia elaeagnoidea* mediated synthesis of silver and gold nanoparticles: Antioxidant and catalysis properties. *J. Clust. Sci.*, 28: 2041-2056.

Mcconnachie, A.J., L.W. Strathie, W. Mersie, L. Gebrehiwot, K. Zewdie, A. Abdurehim, B. Abrha, T. Araya, F. Asaregew and F. Assefa. 2011. Current and potential geographical distribution of the invasive plant *Parthenium hysterophorus* (Asteraceae) in Eastern and Southern Africa. *Weed Res.*, 51: 71-84.

Mobarak, M., M.A. Zied, M. Mostafa and M. Ashari. 2020. Effects of growth technique on the microstructure of CuInSe2 ternary semiconductor compound. *Heliyon*., 6: doi:10.1016/j.heliyon.2020.e03196.

Mohanpuria, P., N.K. Rana and S.K.Yadav. 2008. Biosynthesis of nanoparticles: technological concepts and future applications. *J. Nanopart. Res.*, 10: 507-517.

Moreno, G.U.N.M. de S.M. 2018. Efecto de La Germinación de Tres Variedades de Quinua: Roja (INIA-415 Pasankalla), Negra (INIA 420-Negra Collana) y Blanca (Salcedo INIA) En La Formulación y Elaboración de Una Bebida Funcional Con Capacidad Antioxidante, Universidad Nacional Mayor de San Marcos, Vol. 447. doi:10.18271/ria.2015.109

Mostafa, M., Z.A. Alrowaili, G.M. Rashwan and M.K. Gerges. 2020. Ferroelectric behavior and spectroscopic properties of la-modified lead titanate nanoparticles prepared by a Sol-Gel Method. *Heliyon*., 6: doi:10.1016/j.heliyon.2020.e03389.

Nasiriboroumand, M., M. Montazer and H. Barani. 2018. Preparation and characterization of biocompatible silver nanoparticles using pomegranate peel extract. *J. Photochem. Photobiol. B Biol.*, 179: 98-104.

Nattero, J. and A.A. Cocucci. 2007. Cocucci, geographical variation in floral traits of the tree tobacco in relation to its hummingbird pollinator fauna. *Biol. J. Linn. Soc.*, 90: 657-667.

Oluwaniyi, O.O., H.I. Adegoke, E.T. Adesuji, A.B. Alabi, S.O. Bodede, A.H. Labulo and C.O. Oseghale. 2016. Biosynthesis of silver nanoparticles using aqueous leaf extract of *Thevetia peruviana* Juss and its antimicrobial activities. *Appl. Nanosci.,* 6: 903-912.

Pourzahedi, L., M. Vance and M.J. Eckelman. 2017. Life cycle assessment and release studies for 15 nanosilver-enabled consumer products: Investigating hotspots and patterns of contribution. *Environ. Sci. Technol.,* 51: 7148-7158.

Pujol, I., J. Guarro, C. Llop, L. Soler and J. Fernández-Ballart. 1996. Comparison study of broth macrodilution and microdilution antifungal susceptibility tests for the filamentous fungi. *Antimicrob. Agents Chemother.*, 40: 2106-2110.

Rawat, Y.S., V.S. Negi, S. Pant and R.K. Bachheti. 2023. Collaborative adaptive stewardship for invasive alien plants management in South Africa. *Sustainability*, 15: 4833, doi:10.3390/su15064833.

Rawat, Y.S. 2017. Sustainable biodiversity stewardship and inclusive development in South Africa: A Novel Package for a Sustainable Future. *Curr. Opin. Environ. Sustain.*, 24: 89-95.

Roy, S.T. 2015. Das plant mediated green synthesis of silver nanoparticles-a review. *Int. J. Plant Biol., Res*., 3: 1044-1055.

Salayová, A., Z. Bedlovičová, N. Daneu, M. Baláž, Z.L. Bujňáková, L. Balážová and L. Tkáčiková. 2021. Green synthesis of silver nanoparticles with antibacterial activity using various medicinal plant extracts: Morphology and antibacterial efficacy. *Nanomaterials*, 11(4): p.1005. doi: 10.3390/nano11041005

Scharenberg, F., T. Stegemann, S.S. Çiçek and C. Zidorn, 2019. Sequestration of pyridine alkaloids anabasine and nicotine from nicotiana (Solanaceae) by *Orobanche ramosa* (Orobanchaceae). *Biochem. Syst. Ecol.*, 86: doi:10.1016/ j.bse. 2019. 05.016.

Shu, M., F. He, Z. Li, X. Zhu, Y. Ma, Z. Zhou, Z. Yang, F. Gao and M. Zeng. 2020. Biosynthesis and antibacterial activity of silver nanoparticles using yeast extract as reducing and capping agents. *Nanoscale Res. Lett.*, 15: 1-9, doi:10.1186/ s11671-019-3244-z.

Singh, J., A. Kumar, A.S. Nayal, S. Vikal, G. Shukla, A. Singh, A. Singh, S. Goswami, A. Kumar and Y.K. Gautam. 2024. Comprehensive antifungal investigation of green synthesized silver nanoformulation against four agriculturally significant fungi and its cytotoxic applications. *Sci. Rep.*, 14: doi:10.1038/s41598-024-56619-9.

Singh, H., J. Du, P. Singh and T.H. Yi. 2018. Ecofriendly synthesis of silver and gold nanoparticles by *Euphrasia officinalis* leaf extract and its biomedical applications. *Artif Cells Nanomed Biotechnol*., 46: 1163-1170.

Singh, P., S. Ahn, J.P. Kang, S. Veronika, Y. Huo, H. Singh, M. Chokkaligam, M. El-Agamy Farh, V.C. Aceituno,H.P. Singh, D.R. Batish, J.K. Pandher and R.K. Kohli. 2003. Assessment of ALLELOPATHIC PROPERTIES of *Parthenium hysterophorus* Residues. *Agric. Ecosyst. Environ.*, 95: 537-541, doi:10.1016/S0167-8809(02)00202-5.

Souza, T.G.F., V.S.T. Ciminelli and N.D.S. Mohallem. 2016. A comparison of TEM and DLS methods to characterize size distribution of ceramic nanoparticles. In *Proceedings of the Journal of Physics*: *Conference Series*., Vol. 733. doi:10.1088/1742-6596/733/1/012039

Suganthy, N., V. Sri Ramkumar, A. Pugazhendhi, G. Benelli and G. Archunan. 2018. Biogenic synthesis of gold nanoparticles from *Terminalia Arjuna* bark extract: Assessment of safety aspects and neuroprotective potential via antioxidant, anticholinesterase, and antiamyloidogenic effects. *Environ. Sci. Pollut. Res.*, 25: 10418-10433.

Tamado, T. and P. Milberg. 2000. Weed flora in arable fields of eastern ethiopia with emphasis on the occurrence of *Parthenium hysterophorus*. *Weed Res.*, 40: 507-521, doi:10.1046/j.1365-3180.2000.00208.x.

Thomas, J., M.A. El-Sheikh, A.H. Alfarhan, A.A. Alatar, M. Sivadasan, M. Basahi, S. Al-Obaid and R. Rajakrishnan. 2016. Impact of alien invasive species on habitats and species richness in Saudi Arabia. *J. Arid Environ.*, 127: 53-65.

Vance, M.E., T. Kuiken, E.P. Vejerano, S.P. McGinnis, M.F. Hochella Jr, D. Rejeski and M.S. Hull. 2015. Nanotechnology in the real world: Redeveloping the nanomaterial consumer products inventory. *Beilstein J. Nanotechnol.*, 6: 1769-1780.

Wang, X., L. Yuan, H. Deng and Z. Zhang. 2021. Structural characterization and stability study of green synthesized starch stabilized silver nanoparticles loaded with isoorientin. *Food Chem.*, 338: 127807.